HHS Public Access

Author manuscript

Methods. Author manuscript; available in PMC 2017 April 15.

Published in final edited form as:

Methods. 2016 April 15; 99: 128–134. doi:10.1016/j.ymeth.2015.08.014.

Bioengineering functional human sphincteric and non-sphincteric gastrointestinal smooth muscle constructs

Stephen L Rego[1], **Elie Zakhem**[1,3], **Giuseppe Orlando**[2], and **Khalil N Bitar**[1,3,4]

Stephen L Rego: srego@wakehealth.edu; Elie Zakhem: ezakhem@wakehealth.edu; Giuseppe Orlando: gorlando@wakehealth.edu; Khalil N Bitar: kbitar@wakehealth.edu

[1]Wake Forest Institute for Regenerative Medicine, Wake Forest School of Medicine, Winston-Salem, NC

[2]Department of General Surgery, Wake Forest School of Medicine, Winston-Salem NC

[3]Department of Molecular Medicine and Translational Sciences, Wake Forest School of Medicine, Winston Salem, NC

[4]Virginia Tech-Wake Forest School of Biomedical Engineering and Sciences, Winston Salem, NC

Abstract

Digestion and motility of luminal content through the gastrointestinal (GI) tract are achieved by cooperation between distinct cell types. Much of the 3 dimensional (3D) *in vitro* modeling used to study the GI physiology and disease focus solely on epithelial cells and not smooth muscle cells (SMCs). SMCs of the gut function either to propel and mix luminal contents (phasic; non-sphincteric) or to act as barriers to prevent the movement of luminal materials (tonic; sphincteric). Motility disorders including pyloric stenosis and chronic intestinal pseudoobstruction (CIPO) affect sphincteric and non-sphincteric SMCs, respectively. Bioengineering offers a useful tool to develop functional GI tissue mimics that possess similar characteristics to native tissue. The objective of this study was to bioengineer 3D human pyloric sphincter and small intestinal (SI) constructs *in vitro* that recapitulate the contractile phenotypes of sphincteric and non-sphincteric human GI SMCs. Bioengineered 3D human pylorus and circular SI SMC constructs were developed and displayed a contractile phenotype. Constructs composed of human pylorus SMCs displayed tonic SMC characteristics, including generation of basal tone, at higher levels than SI SMC constructs which is similar to what is seen in native tissue. Both constructs contracted in response to potassium chloride (KCl) and acetylcholine (ACh) and relaxed in response to vasoactive intestinal peptide (VIP). These studies provide the first bioengineered human pylorus constructs that maintain a sphincteric phenotype. These bioengineered constructs provide appropriate models to study motility disorders of the gut or replacement tissues for various GI organs.

Corresponding Author: Khalil N. Bitar, PhD AGAF, 391 Technology Way, Richard H Dean Biomedical Engineering Building, Winston-Salem NC 27101, Phone: (336) 713-1470, Fax: (336) 713-7290, kbitar@wakehealth.edu.

Keywords

bioengineering; gastrointestinal; smooth muscle cells; pylorus

1. Introduction

The gastrointestinal (GI) tract is a tubular hollow organ composed of an array of cell types, including smooth muscle cells (SMCs), neurons, interstitial cells of Cajal (ICC) and epithelial cells, which cooperate to support peristalsis, secretion, digestion, and absorption [1–4]. The majority of current *in vitro* 3D models study GI development, physiology and disease of only the epithelium (mucosa), which covers the lumen of the gut and has primary roles in secretion of digestive enzymes and absorption of nutrients [5–12]. Motility of luminal contents is carried out by SMCs that surround the mucosa, which receives input from neurons and ICCs [13–15]. SMCs are considered as the basic functional units that perform contraction and relaxation. Numerous GI diseases including pyloric stenosis [16, 17] and chronic intestinal pseudoobstruction (CIPO) [18, 19] affect SMCs of the gut leading to dysmotility. There are few 3D functional models that accurately recapitulate the phenotypic and functional characteristics of SMCs within the gut. Of the studies that have investigated functional enteric SMCs *in vitro* the use of decellularized scaffolds [20–23] or collagen sponges [24–27] have been the most successful, highlighting the importance of the extracellular matrix in generating functional 3D models.

GI SMCs can be isolated from the gut, expanded and cultured *in vitro*, however, over time SMCs will lose their characteristic contractile phenotype and acquire a synthetic phenotype in culture [28–30]. A contractile SMC phenotype is characterized by expression of SMC markers including smoothelin, α smooth muscle actin (SMA), caldesmon and calponin along with decreased migration and proliferation of cells [29, 31]. SMCs that have acquired a synthetic phenotype will down regulate SMC markers and begin to migrate and proliferate [29, 32]. This makes *in vitro* studies of SMC physiology and dysfunction more challenging. In this study, we provide a bioengineering approach to construct smooth muscle constructs using primary isolated human SMCs providing a platform to better understand the phenotype of SMCs *in vitro*.

SMCs of the GI tract display sub-phenotypes that can be either tonic (sphincteric) or phasic (non-sphincteric). Sphincters, such as the lower esophageal sphincter (LES), pylorus and internal anal sphincter (IAS), are tonically contracted and ensure unidirectional movement of luminal content through the GI tract. Proteins involved in tonic contraction of SMCs include C-kinase potentiated protein phosphatase-1 inhibitor (CPI-17), Ras homolog gene family member A (RhoA) and Rho-associated protein kinase II (ROCKII) [13, 33, 34]. When appropriate signals are received, the sphincters relax and allow passage of the luminal content. Phasic SMCs, such as those found in the lower part of the esophagus, stomach, small intestine (SI) and colon, mediate peristalsis through rhythmic segmentation of the gut wall to propel materials in an aboral direction. SMCs also facilitate mixing of the luminal contents [32, 35–38]. Currently, there are no *in vitro* systems that recapitulate and compare the characteristics of both smooth muscle sub-phenotypes.

The objective of this study was to utilize bioengineering techniques to develop 3D *in vitro* models that appropriately recapitulate the contractile phenotypes of sphincteric and non-sphincteric human GI SMCs. In this study, human pylorus-derived SMCs were used to bioengineer 3D sphincteric constructs and SI-derived SMCs were used to bioengineer 3D non-sphincteric constructs and these constructs were compared using biochemical and physiological assays.

2. Material and Methods

2.1. Reagents

Culture media reagents were purchased from Invitrogen (Carlsbad, CA) unless otherwise specified. Growth media for SMCs contained Dulbecco's Modified Eagle Medium (DMEM) with 10% fetal bovine serum (FBS), 1X antibiotics-antimycotics, and L-glutamine. Growth media for neurospheres contained Neurobasal (Life Technologies, Grand Island, NY), 1X N2 supplement (Life Technologies), 20 ng/mL recombinant human Epidermal Growth Factor (EGF, Stemgent, San Diego, CA), 20 ng/mL recombinant basic Fibroblast Growth Factor (bFGF, Stemgent, San Diego, CA) and 1X antibiotics. Differentiation media contained Neurobasal-A (Life Technologies), 1X B27 supplement (Life Technologies), 2% FBS and 1X antibiotics [39]. Rat tail collagen Type I was purchased from BD Biosciences (Bedford, MA), dispase and DNAse from Roche Applied Science (Indianapolis, IN), collagenase from Worthington Biochemicals (Lakewood, NY) and Hank's Balanced Salt Solution (HBSS) from Thermo Scientific HyClone (Logan, UT).

2.2. Isolation of smooth muscle cells from human pyloric sphincters and small intestines

Human pylorus and intestinal tissues were obtained through Carolina Donor Services and Wake Forest Baptist Medical Center (IRB#: IRB00007586) in accordance with The Code of Ethics of the World Medical Association. Sphincteric smooth muscle cells were obtained from the pyloric sphincter and SI smooth muscle cells were consistently obtained from the duodenum. SMCs were isolated from human GI tissues as described previously [40, 41]. Briefly, pylorus and SI tissues were removed by sharp dissections and manually cleaned by removing fat and mucosa with a surgical blade. Tissue were washed in ice-cold HBSS solution containing 2X antibiotics-antimycotics 5 times, minced in sterile conditions and again washed with sterile HBSS. Tissues were digested twice in HBSS with 0.1% collagenase type II (Worthington Biochemical, Lakewood, NJ) at 37°C with agitation for 1 hour. After the second digest, samples were centrifuged at 600 g for 10 min, and the supernatant was discarded. The cells were washed, resuspended in SMC growth media, placed in tissue culture dishes and incubated at 37°C with 5% CO_2.

2.3. Bioengineered circular SMC constructs

Bioengineering pylorus (n=3) and SI (n=3) SI SMC constructs were generated utilizing similar methods described previously to generate IAS constructs [41, 42]. Three replicates were performed for each experiment on the bioengineered constructs generated from different patients. Human SMCs cultured for less than 4 passages were used in constructs. Sylgard coated 35-mm culture dishes were used with an 8 mm diameter central Sylgard post. SMCs were enzymatically detached with trypsin and counted using a hemacytometer.

500,000 SMCs (either pylorus or SI) were resuspended in 1 mL of 0.8 mg/mL Collagen I solution in 1X DMEM with 10% FBS and 1X antibiotics-antimycotics. This collagen I SMC solution was placed on Sylgard coated plates with central Sylgard posts and allowed to gel for 1 hour. 1 mL of SMC differentiation media was added to constructs which were incubated at 37°C and 5% CO_2. By day 3 SMCs contracted around central Sylgard posts forming circular tissues with an internal diameter of 8 mm. Every other day media was aspirated and 1 mL of fresh differentiation media added.

2.4. Immunoblot analyses

Confluent monolayer cultures (2D) or days 10–12 bioengineered constructs (3D) were harvested for analysis. Lysates were collected in radioimmunoprecipitation assay (RIPA) buffer and immunodetection performed as described earlier [43, 44]. Briefly, 30 μg of total protein were loaded on 8% polyacrylamide gels and separated with SDS-PAGE. Proteins were then transferred onto polyvinylidene difluoride (PVDF) membranes and even loading determined by ponceau S (0.1%, SigmaAldrich, St Louis, MO, USA) staining. Membranes were incubated with 1X Tris-buffered saline-0.1% Tween 20 (TBS-T) containing 5% nonfat milk, then incubated with antibodies specific for smoothelin (abcam, Cambridge, MA, USA), caldesmon, SMA, β-actin (SigmaAldrich, St Louis, MO, USA) CPI-17, phosphorylated CPI-17 (pCPI-17), RhoA or ROCKII (EMD Millipore, Billerica, Massachusetts, USA). Unbound antibodies were removed by washing, then membranes were incubated with appropriate horseradish peroxidase (HRP) conjugated secondary antibody. Antibody-bound proteins were detected using HyGLO chemiluminescent HRP reagent (Denville Scientific Inc, South Plainfield, NJ, USA) and pictures taken with a chemiluminescent imaging system (FujiFilm LAS-3000).

2.5. Immunohistochemical characterization of smooth muscle cells within bioengineered constructs

Immunohistochemical (IHC) staining was performed following previously established protocols for staining bioengineered tissues [41, 43]. Bioengineered constructs at days 10–12 were fixed in 3.7% formaldehyde, embedded in paraffin and 6 μm sections placed on microscope slides. Slides were washed in glycine buffer, blocked and permeabilized with 10% horse serum with 0.15% Triton-X for 45 min. Hematoxilin and eosin (H&E) staining was performed or slides were incubated in primary antibodies for caldesmon, calponin and SMA (SigmaAldrich, St Louis, MO, USA) for one hour at room temperature. Appropriate FITC-conjugated secondary antibodies were then applied for 30 minutes and slides were mounted using VECTASHIELD (Vector Laboratories Inc., Burlingame, CA). Negative controls were prepared to assess background by incubation with only fluorophore conjugated secondary antibodies. Cells were visualized using an inverted Nikon Ti-E fluorescence microscope (Nikon, Japan).

2.6. Physiological testing of bioengineered constructs

Myogenic functionality tests were performed as described previously [28]. At days 10–12, sphincteric and non-sphincteric SMC constructs were hooked to an isometric, magnetoresistive force transducer (F10; Harvard Apparatus, Holliston, MA) and data acquired using LabScribe2 software (iWorx, Han-over, NH). SMC constructs were

immersed in sterile DMEM with HEPES medium maintained at 37°C. Generation of a spontaneous basal tone was assessed on tissues after applying a 20% stretch and allowing tissues to equilibrate to a stable base line. Basal tone values are reported as average delta force values after tissues stabilize (1–2 minutes) without any normalization. 20% stretch was maintained during the testing period. Contraction and relaxation were evaluated with the addition of ACh (1 μM) and KCl (60 mM) or VIP (1 μM), respectively. ACh response was additionally evaluated in the presence of muscarinic receptor antagonist, atropine (1 μM). Constructs were treated with 1 μM atropine for 5 minutes followed by administration of the same dose of ACh. Data analysis was performed using GraphPad Prism 5.01 software for Windows (GraphPad Software, San Diego CA; www.graphpad.com). Second-order Savitsky–Golay smoothing was applied and values were expressed as means and standard error of the mean (SEM) of at least three experiments. The quantitative measure used for force generation studies was maximum or minimum delta force (μNewtons) unless otherwise specified.

2.7. Statistical analyses

Data was expressed as mean ± SEM using GraphPad software (Prism, Graphpad Software, Inc., La Jolla, CA, USA) unless specified otherwise. One-way ANOVAs and Newmann-Keul post-hoc tests were used to determine differences between experimental groups. Significance was set to p values below 0.05.

3. Results and Discussion

3.1. Characterization of contractile protein expression in bioengineered human smooth muscle constructs with sphincteric and non-sphincteric cells through immunoblot analysis

Bioengineered human constructs composed of pylorus (sphincteric) and small intestines (SI; non-sphincteric) SMCs formed compacted rings after 4 days in culture (Figure 1A). Neural cells and interstitial cells were not present in these constructs. These constructs were assessed for expressions of smooth muscle markers including, caldesmon, smoothelin and SMA utilizing immunoblot analysis to determine whether they maintained a contractile smooth muscle phenotype. β-actin expression was determined to ensure equal loading. All constructs demonstrated positive expression of caldesmon, smoothelin and SMA confirming the presence of SMCs with a contractile phenotype (Figure 1B). Smoothelin expression between confluent monolayer cultures (2D) and bioengineered constructs (3D) was compared utilizing immunoblots. Higher levels of smoothelin were observed in bioengineered pylorus and SI constructs (3D) compared to monolayer pylorus and SI SMCs, respectively (Figure 2C) indicating the SMCs within these bioengineered constructs demonstrated a superior contractile phenotype compared to 2D SMC cultures. This is the first instance of a bioengineered 3D *in vitro* human pylorus constructs. Furthermore, SMCs tend to lose their contractile phenotype once in culture [29], however, within these bioengineered constructs they are shown to maintain expression of SMC markers and contractile proteins for at least 12 days *in vitro* at higher levels than 2D cultured SMCs.

3.2. Alignment and SMC marker expression of sphincteric and non-sphincteric bioengineered human smooth muscle constructs assessed through immunohistochemical analysis

H&E staining was performed on bioengineered human pylorus and SI SMC constructs to determine orientation of SMCs. Both bioengineered pylorus and SI constructs demonstrated circumferential alignment (Figure 2). To further assess the expression of SMC markers, immunofluorescence studies were performed on paraffin sections of constructs. Expression of common SMC markers SMA, caldesmon and calponin, were observed in bioengineered human pylorus and SI constructs (Figure 2). No positive staining was observed by constructs incubated with secondary antibody alone indicating this signal was due to specific binding to primary antibodies. These results further verify the maintenance of a contractile SMC phenotype by demonstrating preservation of SMC markers. Synthetic SMCs lack the expression of these markers and express proteins involved in proliferation and migration [30, 45].

3.3. Physiologic and biochemical assessment of tonic smooth muscle cell characteristics displayed by bioengineered human pylorus and small intestine-derived smooth muscle constructs

To assess the functionality of bioengineered human sphincteric and non-sphincteric SMC constructs, real time force generation studies were performed. The generation of a spontaneous basal tone was assessed after applying 20% stretch to the tissues with no other external stimuli. After tissues stabilized average delta force values were calculated and reported as basal tone. Bioengineered human pylorus constructs generated a robust basal tone with an average maximum delta force of 500 μNewtons (SEM = 55.9, Figure 3A) while human SI constructs produced weaker basal forces averaging 23.7 μNewtons (SEM = 6.9, Figure 3B). Basal tones generated by bioengineered human pylorus constructs were significantly higher than the maximum force generated by bioengineered human SI constructs (***$p<0.001$, $n=3$, Figure 3C). Obtaining intact functional human pylorus tissue to compare the basal tone of our bioengineered tissues was not possible in this study. However, future studies are being planned to investigate the relative level of basal tone produced by bioengineered constructs compared to native tissue which will assist in determining parameters for scaling up constructs to serve as models with comparable basal tone to native tissue. This will present the next step towards generating functional replacement organs.

Immunoblot analyses were performed to compare expression levels of proteins involved in tonic SMC activities including, ROCKII, RhoA, pCPI-17 and CPI-17. ROCKII, RhoA, pCPI-17 and CPI-17 were all expressed at higher levels in human pylorus SMC constructs compared to SI constructs. These studies further validate the ability of SMCs within these bioengineered constructs to maintain a distinctive sphincteric or non-sphincteric phenotype. This supports the relevance of bioengineered SMC tissues as models to study and compare GI sphincteric and non-sphincteric SMCs *in vitro*. Maintaining the expression of the machinery involved in tonic SMC contraction is another step forward in the bioengineering of functional GI SMC tissues. Studies utilizing typical 2D cultures are problematic in that SMCs lose their contractile characteristics. Furthermore, bioengineered human SMC

constructs have the potential to serve as functional replacement organs for various regions of the GI tract, including sphincteric and non-sphincteric regions.

3.4. Physiologic assessment of force generation by bioengineered human pylorus and small intestine-derived smooth muscle constructs in response contractile stimuli

To further assess the contractile SMC activity of bioengineered human sphincteric and non-sphincteric constructs, real-time force generation measurements were obtained after treatment with KCl and ACh. 60 mM KCl (arrow) induced a robust contraction in sphincteric and non-sphincteric constructs (Figure 4 A and B). A significant increase in the maximum force of contraction in response to KCl was observed in bioengineered human pylorus constructs (519 μNewtons ± 19.97) compared to SI constructs (411 μNewtons ± 32.48, *$p<0.05$, n=3, Figure 4C). Constructs were washed and allowed to establish baseline before treating with ACh. Similarly to KCl, both bioengineered constructs demonstrated robust contractions in response to ACh (pylorus; 184.90 μNewtons ± 5.66, n=3, SI; 172.1 μNewtons ± 2.37, n=3, Figure 4D–F). Constructs were washed with fresh buffer and allowed to establish baseline again. Both constructs were then treated with 1 μM atropine for 5 minutes before the addition of 1 μM ACh. Contraction in response to Ach was abolished in the presence of atropine (Figure 4D & E, red trace). ACh acts on the smooth muscle cells by blocking muscarinic receptors, leading to inhibition of contraction [46, 47]. The inhibition of Ach-induced contraction in the presence of atropine indicated the preservation of functional muscarinic receptors in bioengineered constructs. Analysis of ACh induced contraction between bioengineered human pylorus and SI constructs indicated no significant differences in maximum force of contraction (Figure 4F). These results demonstrate the ability of bioengineered human SMC constructs to contract in response to exogenous contractile stimuli. The increased force of contraction of bioengineered human pylorus constructs compared to SI constructs may be due to the distinct contractile machinery used by sphincteric and non-sphincteric GI SMCs [33].

3.5. Physiologic assessment of force generation by bioengineered human pylorus and small intestine-derived smooth muscle constructs in response relaxant stimulus, vasoactive intestinal peptide

We further assessed whether the bioengineered human SMC constructs have the potential to relax in response to VIP. VIP caused relaxation in all constructs tested (Figure 5). Bioengineered human pylorus constructs produced on average a maximal relaxation force of −222.7 μNewtons (SEM = 4.61, n=3, Figure 5A and C) and human SI constructs produced a maximal relaxation force of −208.6 μNewtons (SEM = 6.76, n=3, Figure 5B and C) which were not significantly different. These functional analyses of bioengineered GI SMC constructs demonstrated their ability to contract and relax in response to physiologic stimuli. Bioengineered tissues have the advantage of providing functional tissues that may serve as organ replacements. Additionally, they provide an *in vitro* model to study complex physiologic processes that are not recapitulated in a 2D setting. Insights into specific signaling pathways involved in the contraction and relaxation of sphincteric and non-sphincteric GI SMCs can be gained utilizing the bioengineered tissues described here. Furthermore, these constructs provide a platform for investigators to study the interactions between gut derived SMCs and others cells in the GI tract, such as neurons, epithelial cells

and immune cells. These interactions shape gut activities, including differentiation, motility and digestion, and are especially important in responding to stress and insult [48–51]. Utilizing these bioengineered constructs investigators can begin to identify additional mechanisms that distinguish tonic and phasic SMCs and begin to study whether cell-cell interactions vary depending on the origin of SMCs (sphincteric or non-sphincteric) used in bioengineered constructs.

4. Conclusions

Bioengineering techniques provide useful platforms to generate replacement organs as well as study cellular behaviors in a more appropriate 3D context. Here methods to generate functional 3D bioengineered human GI pylorus and SI SMC constructs that maintain contractile phenotypes along with distinctive sphincteric and non-sphincteric phenotypes, respectively, are presented. This is the first instance where a bioengineered human pylorus is generated and these pyloric constructs were shown to maintain a distinct phenotype when compared to bioengineered SI SMC constructs. Future studies investigating SMC intrinsic cellular behaviors as well as interactions with other cells utilizing these constructs are warranted. Furthermore, these miniature phenotypic replicas of native human GI tissues also have applications in larger efforts to develop a “body on a chip”, including investigating the effects of chemical agents on GI motility.

Acknowledgments

This work was supported by Army, Navy, NIH, Air Force, VA and Health Affairs to support the AFIRM II effort, under Award No. W81XWH-13-2-0052; GU 7 and NIH/NIDDK R01DK071614

Abbreviations

GI	gastrointestinal
SMCs	smooth muscle cells
CIPO	chronic intestinal pseudoobstruction
SI	small intestine
KCl	potassium chloride
ACh	acetylcholine
VIP	vasoactive intestinal peptide
SMA	α smooth muscle actin
LES	lower esophageal sphincter
IAS	internal anal sphincter
DMEM	Dulbecco’s Modified Eagle Medium
FBS	fetal bovine serum
EGF	Epidermal Growth Factor

bFGF	basic Fibroblast Growth Factor
HBSS	Hank's Balanced Salt Solution
RIPA	radioimmunoprecipitation assay
PVDF	polyvinylidene difluoride
TBS-T	Tris-buffered saline-0.1% Tween 20
HRP	horseradish peroxidase
IHC	immunohistochemical
H&E	Hematoxilin and eosin
SEM	standard error of the mean

References

1. Bitar KN, Zakhem E. Tissue engineering and regenerative medicine as applied to the gastrointestinal tract. Curr Opin Biotechnol. 2013; 24(5):909–915. [PubMed: 23583170]
2. Van de Graaff KM. Anatomy and physiology of the gastrointestinal tract. Pediatr Infect Dis. 1986; 5(1 Suppl):S11–S16. [PubMed: 3945583]
3. van den Brink GR. Hedgehog signaling in development and homeostasis of the gastrointestinal tract. Physiol Rev. 2007; 87(4):1343–1375. [PubMed: 17928586]
4. Gershon MD. V. Genes, lineages, and tissue interactions in the development of the enteric nervous system. Am J Physiol. 1998; 275(5 Pt 1):G869–G873. [PubMed: 9815012]
5. Mahe MM, et al. Establishment of gastrointestinal epithelial organoids. Curr Protoc Mouse Biol. 2013; 3:217–240. [PubMed: 25105065]
6. McCracken KW, et al. Modelling human development and disease in pluripotent stem-cell-derived gastric organoids. Nature. 2014
7. Sato T, et al. Long-term expansion of epithelial organoids from human colon, adenoma, adenocarcinoma, and Barrett's epithelium. Gastroenterology. 2011; 141(5):1762–1772. [PubMed: 21889923]
8. Sato T, Clevers H. Growing self-organizing mini-guts from a single intestinal stem cell: mechanism and applications. Science. 2013; 340(6137):1190–1194. [PubMed: 23744940]
9. Buske P, et al. On the biomechanics of stem cell niche formation in the gut--modelling growing organoids. FEBS J. 2012; 279(18):3475–3487. [PubMed: 22632461]
10. Tauro BJ, et al. Two distinct populations of exosomes are released from LIM1863 colon carcinoma cell-derived organoids. Mol Cell Proteomics. 2013; 12(3):587–598. [PubMed: 23230278]
11. Hayward IP, et al. Effect of TGF-beta on differentiated organoids of the colon carcinoma cell line LIM 1863. Immunol Cell Biol. 1995; 73(3):249–257. [PubMed: 7590899]
12. Whitehead RH, et al. A new colon carcinoma cell line (LIM1863) that grows as organoids with spontaneous differentiation into crypt-like structures in vitro. Cancer Res. 1987; 47(10):2683–2689. [PubMed: 3567898]
13. Somara S, Gilmont R, Bitar KN. Role of thin-filament regulatory proteins in relaxation of colonic smooth muscle contraction. Am J Physiol Gastrointest Liver Physiol. 2009; 297(5):G958–G966. [PubMed: 20501443]
14. Somara S, et al. Phosphorylated HSP20 modulates the association of thin-filament binding proteins: caldesmon with tropomyosin in colonic smooth muscle. Am J Physiol Gastrointest Liver Physiol. 2010; 299(5):G1164–G1176. [PubMed: 20829522]
15. Somara S, Bitar KN. Direct association of calponin with specific domains of PKC-alpha. Am J Physiol Gastrointest Liver Physiol. 2008; 295(6):G1246–G1254. [PubMed: 18948438]

16. Jenson HB, Gulley ML, Puri P. Absence of Epstein-Barr virus in smooth muscle cells of idiopathic hypertrophic pyloric stenosis. Arch Pathol Lab Med. 2001; 125(3):361–363. [PubMed: 11231484]
17. Oue T, Puri P. Smooth muscle cell hypertrophy versus hyperplasia in infantile hypertrophic pyloric stenosis. Pediatr Res. 1999; 45(6):853–857. [PubMed: 10367777]
18. Mericskay M, et al. Inducible mouse model of chronic intestinal pseudo-obstruction by smooth muscle-specific inactivation of the SRF gene. Gastroenterology. 2007; 133(6):1960–1970. [PubMed: 18054567]
19. De Giorgio R, et al. Advances in our understanding of the pathology of chronic intestinal pseudo-obstruction. Gut. 2004; 53(11):1549–1552. [PubMed: 15479666]
20. Chen MK, Badylak SF. Small bowel tissue engineering using small intestinal submucosa as a scaffold. J Surg Res. 2001; 99(2):352–358. [PubMed: 11469910]
21. Hodde JP, et al. Glycosaminoglycan content of small intestinal submucosa: a bioscaffold for tissue replacement. Tissue Eng. 1996; 2(3):209–217. [PubMed: 19877943]
22. Prevel CD, et al. Small intestinal submucosa: utilization for repair of rodent abdominal wall defects. Ann Plast Surg. 1995; 35(4):374–380. [PubMed: 8585680]
23. Qin HH, Dunn JC. Small intestinal submucosa seeded with intestinal smooth muscle cells in a rodent jejunal interposition model. J Surg Res. 2011; 171(1):e21–e26. [PubMed: 21937060]
24. Nakase Y, et al. Tissue engineering of small intestinal tissue using collagen sponge scaffolds seeded with smooth muscle cells. Tissue Eng. 2006; 12(2):403–412. [PubMed: 16548698]
25. Grikscheit TC. Tissue engineering of the gastrointestinal tract for surgical replacement: a nutrition tool of the future? Proc Nutr Soc. 2003; 62(3):739–743. [PubMed: 14692609]
26. Grikscheit T, Srinivasan A, Vacanti JP. Tissue-engineered stomach: a preliminary report of a versatile in vivo model with therapeutic potential. J Pediatr Surg. 2003; 38(9):1305–1309. [PubMed: 14523810]
27. Grikscheit TC, et al. Tissue-engineered large intestine resembles native colon with appropriate in vitro physiology and architecture. Ann Surg. 2003; 238(1):35–41. [PubMed: 12832963]
28. Patel R, et al. Synthetic smooth muscle cell phenotype is associated with increased nicotinamide adenine dinucleotide phosphate oxidase activity: effect on collagen secretion. J Vasc Surg. 2006; 43(2):364–371. [PubMed: 16476616]
29. Jarrousse C, et al. Cultured gastrointestinal smooth muscle cells: cell response to contractile agonists depends on their phenotypic state. Cell Tissue Res. 2004; 316(2):221–232. [PubMed: 15004749]
30. Bitar KN. Function of gastrointestinal smooth muscle: from signaling to contractile proteins. Am J Med. 2003; 115(Suppl 3A):15S–23S. [PubMed: 12928070]
31. Ehlert FJ, Sawyer GW, Esqueda EE. Contractile role of M2 and M3 muscarinic receptors in gastrointestinal smooth muscle. Life Sci. 1999; 64(6–7):387–394. [PubMed: 10069501]
32. Gerthoffer WT, et al. Myosin phosphorylation and calcium in tonic and phasic contractions of colonic smooth muscle. Am J Physiol. 1991; 260(6 Pt 1):G958–G964. [PubMed: 1905487]
33. Somara S, et al. Bioengineered internal anal sphincter derived from isolated human internal anal sphincter smooth muscle cells. Gastroenterology. 2009; 137(1):53–61. [PubMed: 19328796]
34. Patel CA, Rattan S. Spontaneously tonic smooth muscle has characteristically higher levels of RhoA/ROK compared with the phasic smooth muscle. Am J Physiol Gastrointest Liver Physiol. 2006; 291(5):G830–G837. [PubMed: 16763289]
35. Zhang Y, Hermanson ME, Eddinger TJ. Tonic and phasic smooth muscle contraction is not regulated by the PKCalpha - CPI-17 pathway in swine stomach antrum and fundus. PLoS One. 2013; 8(9):e74608. [PubMed: 24058600]
36. McCarron JG, et al. Agonist-induced phasic and tonic responses in smooth muscle are mediated by InsP(3). J Cell Sci. 2002; 115(Pt 10):2207–2218. [PubMed: 11973361]
37. Uvelius B, Hellstrand P. Effects of phasic and tonic activation on contraction dynamics in smooth muscle. Acta Physiol Scand. 1980; 109(4):399–406. [PubMed: 7468260]
38. Golenhofen K, Weiser HF, Siewert R. Phasic and tonic types of smooth muscle activity in lower oesophageal sphincter and stomach of the dog. Acta Hepatogastroenterol (Stuttg). 1979; 26(3): 227–234. [PubMed: 484172]

39. Raghavan S, Gilmont RR, Bitar KN. Neuroglial differentiation of adult enteric neuronal progenitor cells as a function of extracellular matrix composition. Biomaterials. 2013; 34(28):6649–6658. [PubMed: 23746858]
40. Gan L, et al. Infected peripheral blood mononuclear cells transmit latent varicella zoster virus infection to the guinea pig enteric nervous system. J Neurovirol. 2014
41. Gilmont RR, et al. Bioengineering of physiologically functional intrinsically innervated human internal anal sphincter constructs. Tissue Eng Part A. 2014; 20(11–12):1603–1611. [PubMed: 24328537]
42. Zakhem E, Raghavan S, Bitar KN. Neo-innervation of a bioengineered intestinal smooth muscle construct around chitosan scaffold. Biomaterials. 2014; 35(6):1882–1889. [PubMed: 24315576]
43. Rego SL, et al. Soluble tumor necrosis factor receptors shed by breast tumor cells inhibit macrophage chemotaxis. J Interferon Cytokine Res. 2013; 33(11):672–681. [PubMed: 23777205]
44. Rego SL, Helms RS, Dreau D. Breast tumor cell TACE-shed MCSF promotes pro-angiogenic macrophages through NF-kappaB signaling. Angiogenesis. 2014; 17(3):573–585. [PubMed: 24197832]
45. Boettger T, et al. Acquisition of the contractile phenotype by murine arterial smooth muscle cells depends on the Mir143/145 gene cluster. J Clin Invest. 2009; 119(9):2634–2647. [PubMed: 19690389]
46. Hosey MM, et al. The role of G-protein coupled receptor kinases in the regulation of muscarinic cholinergic receptors. Prog Brain Res. 1996; 109:169–179. [PubMed: 9009704]
47. Lee TP, Kuo JF, Greengard P. Role of muscarinic cholinergic receptors in regulation of guanosine 3':5'-cyclic monophosphate content in mammalian brain, heart muscle, and intestinal smooth muscle. Proc Natl Acad Sci U S A. 1972; 69(11):3287–3291. [PubMed: 4343961]
48. Roberts DJ. Molecular mechanisms of development of the gastrointestinal tract. Dev Dyn. 2000; 219(2):109–120. [PubMed: 11002332]
49. Muller PA, et al. Crosstalk between muscularis macrophages and enteric neurons regulates gastrointestinal motility. Cell. 2014; 158(2):300–313. [PubMed: 25036630]
50. Anderson RB, Newgreen DF, Young HM. Neural crest and the development of the enteric nervous system. Adv Exp Med Biol. 2006; 589:181–196. [PubMed: 17076282]
51. Gershon MD, Chalazonitis A, Rothman TP. From neural crest to bowel: development of the enteric nervous system. J Neurobiol. 1993; 24(2):199–214. [PubMed: 8445388]

Highlights

- Bioengineering human pylorus and small intestine smooth muscle constructs
- Constructs exhibit contractile phenotypes and respond to physiologic stimuli
- Sphincteric and non-sphincteric characteristics are maintained in constructs
- These constructs provide useful models to investigate motility disorders

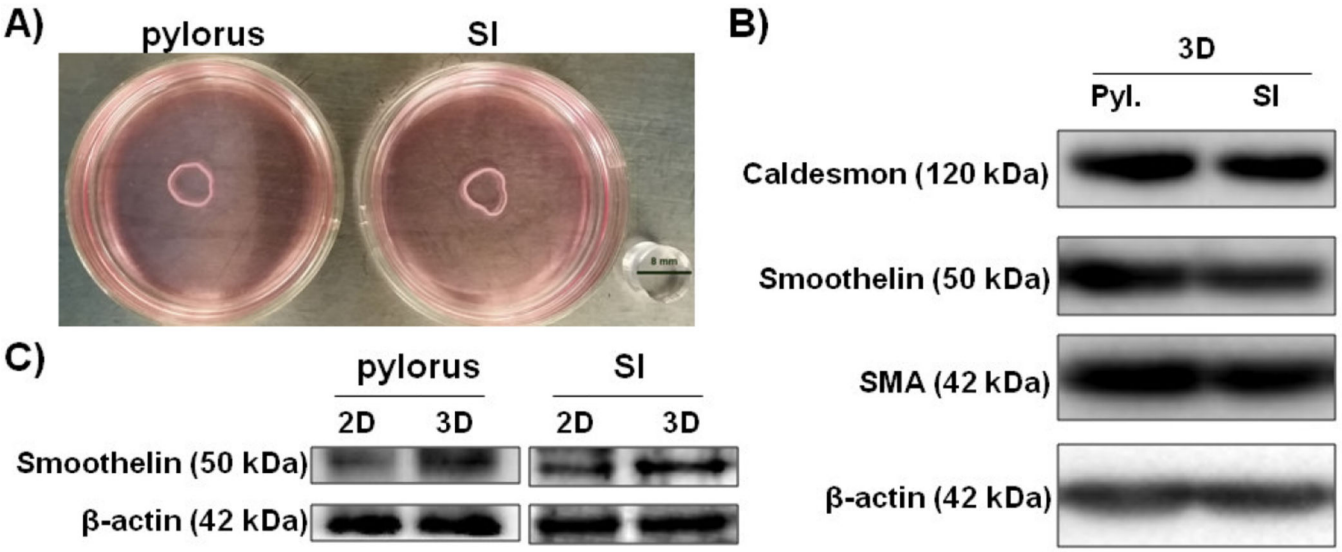

Figure 1. Immunoblot analysis of smooth muscle marker expression in sphincteric and non-sphincteric bioengineered human smooth muscle constructs

A) Bioengineered human pylorus and SI SMC constructs formed concentric rings by day 4. Immunoblot analyses were performed on bioengineered human SMC constructs after 10 days in culture. B) Positive expression of SMC markers Caldesmon, Smoothelin and SMA was observed in all constructs tested. β-actin served as a loading control. C) Higher expression of the contractile SMC marker smoothelin was observed in bioengineered 3D constructs compared to 2D monolayer cultures.

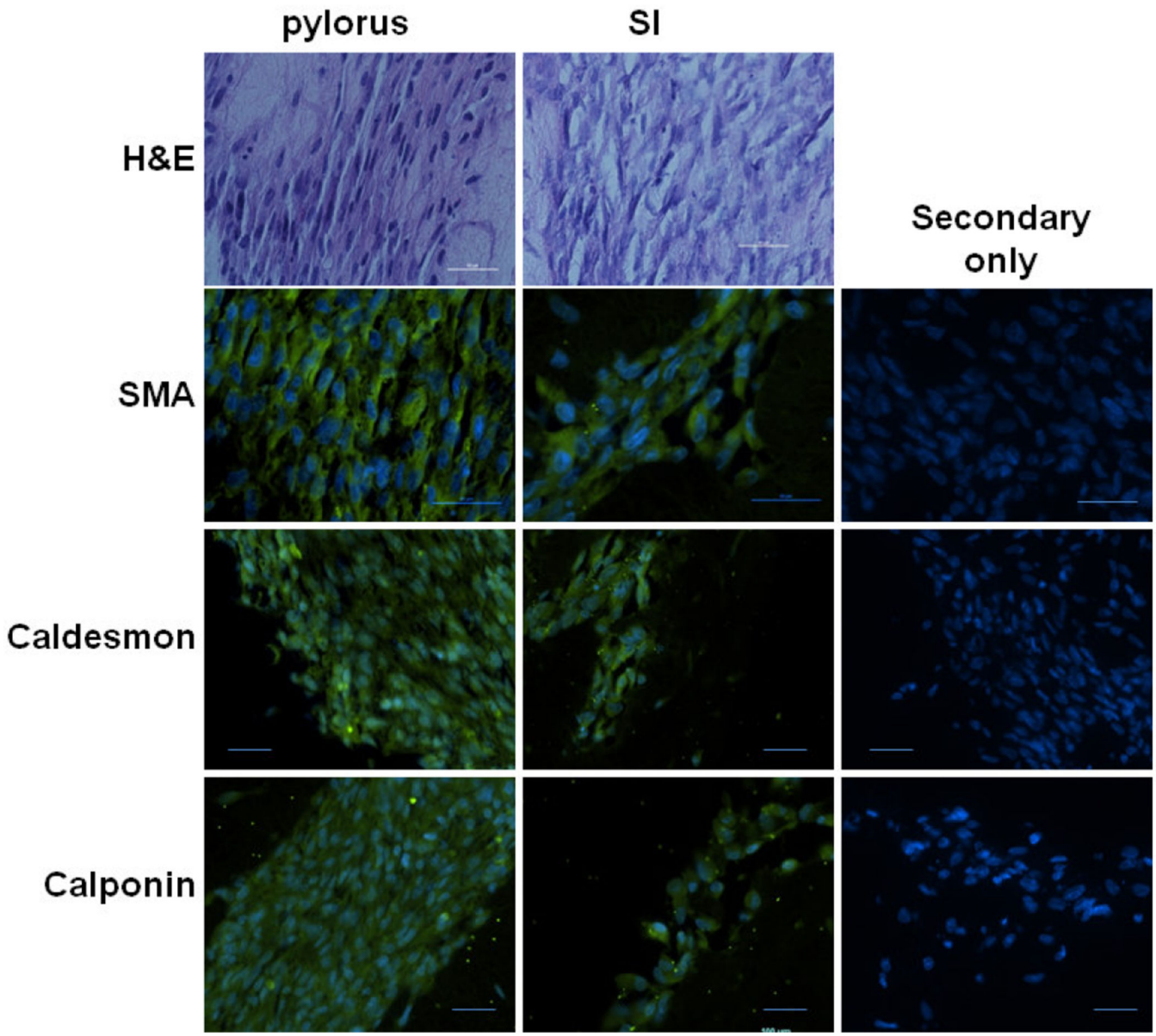

Figure 2. Immunohistochemical analysis of sphincteric and non-sphincteric bioengineered human smooth muscle constructs

Alignment of SMCs within bioengineered constructs was assessed through H&E staining. Both pylorus and SI SMC constructs aligned concentrically. Expression of SMC markers SMA, Caldesmon and Calponin were assessed through immunofluorescence staining. All constructs demonstrated positive expression of SMA, Caldesmon and Calponin. No signal was observed on sections stained with secondary antibody only. All scale bars = 50 μm.

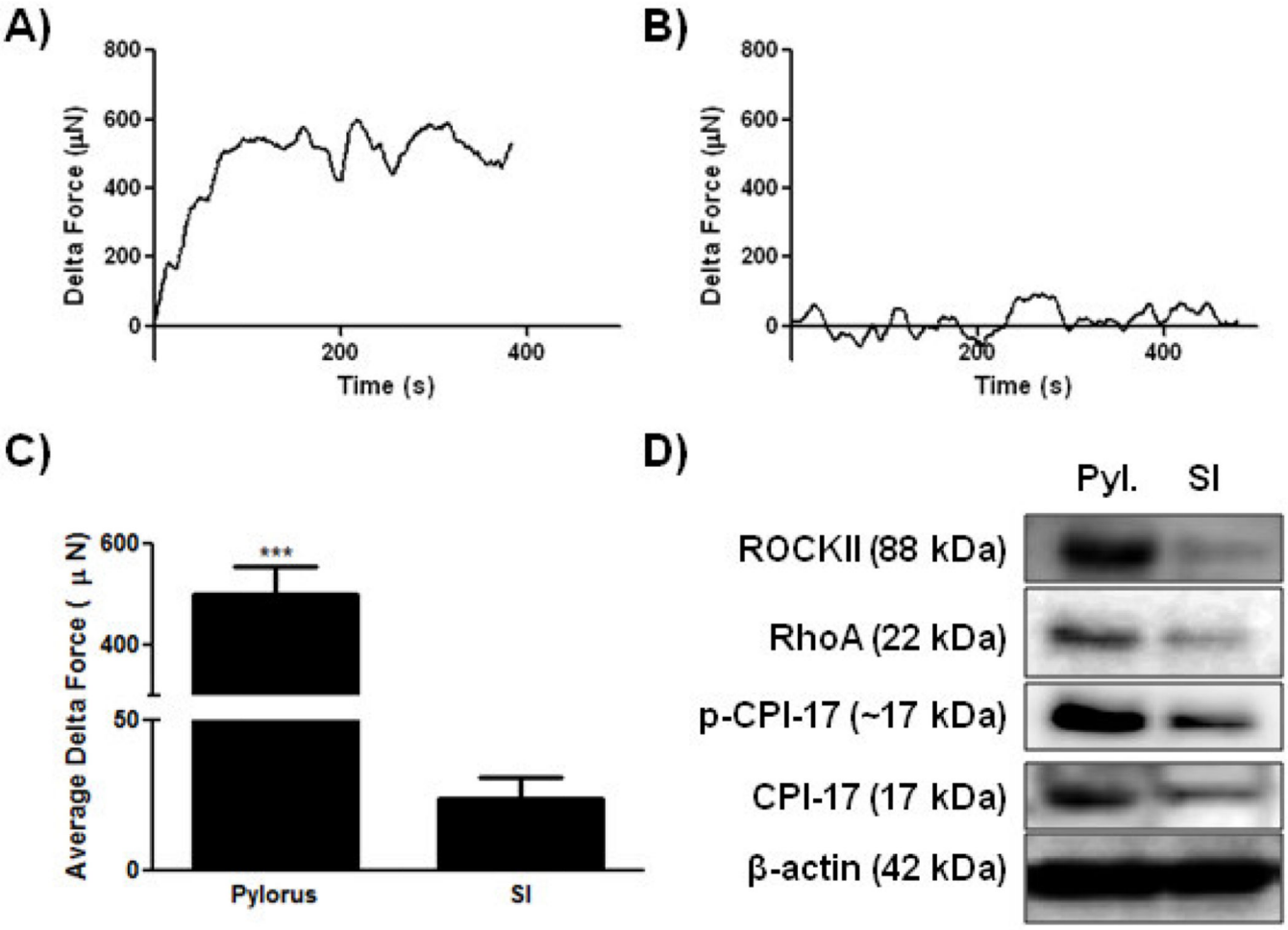

Figure 3. Force generation analysis of tonic smooth muscle characteristics in bioengineered human gastrointestinal smooth muscle constructs

Measurements of spontaneous basal tones were acquired through real time force generation studies. A) and B) Representative tracings of bioengineered human SMC constructs are presented. A) Bioengineered human pylorus constructs produced a robust basal tone with an average delta force after stabilizing of 500 μN (SEM±55.9). B) Bioengineered human SI SMC constructs generated significantly weaker basal forces averaging 23.7 μN (SEM±6.9) when compared to pylorus constructs (***$p<0.001$). C) Comparisons of basal tone generated by human pylorus and SI SMC constructs are presented (n=3). D) Immunoblot analysis of proteins involved in tonic SMC contraction including p-CPI-17, CPI-17 and RhoA demonstrate higher expression levels in human pyloric constructs than SI constructs. β-actin served as a loading control.

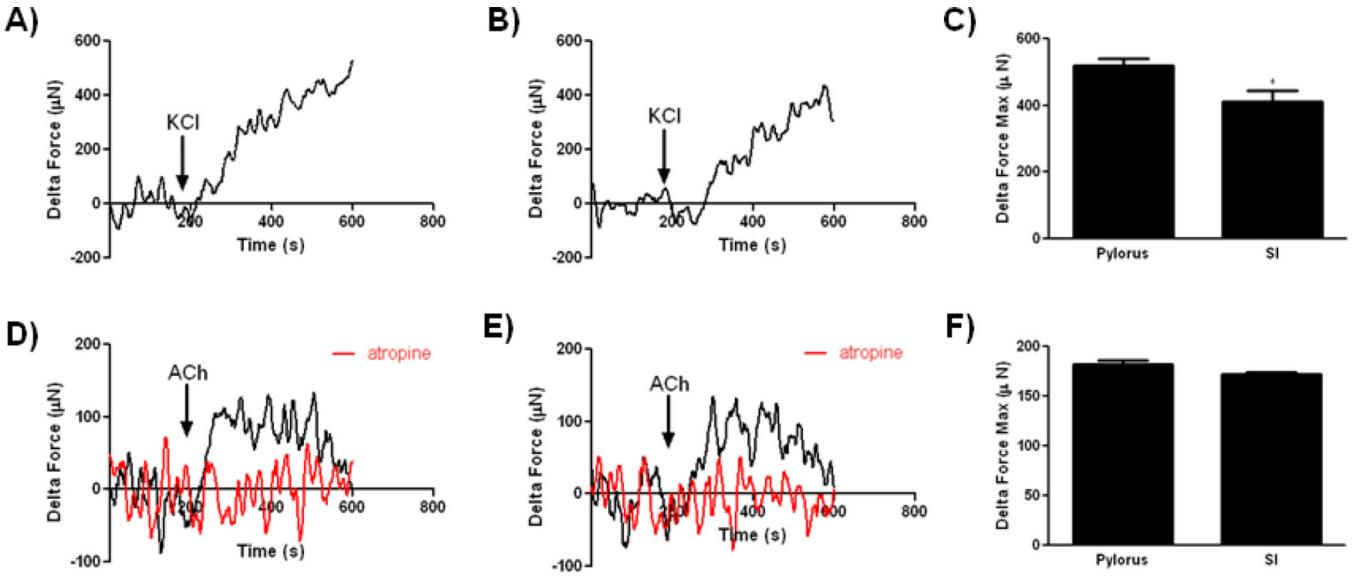

Figure 4. Physiologic assessment of force generation by bioengineered smooth muscle constructs in response to potassium chloride and acetylcholine

Force of contraction measurements were acquired by real time force generation measurements taken after stimulation of constructs with 60 mM KCl or 1 μM ACh. A) Representative tracings of human pylorus SMC constructs are presented. Bioengineered human pylorus constructs produced a robust contraction in response to KCl averaging 519.8 μN (SEM±19.97). B) Human SI SMC constructs also contracted in response to KCl averaging 411.8 μN (SEM±32.48). C) Contraction in response to KCl was significantly higher in bioengineered human pylorus constructs compared to SI constructs (*$p<0.05$, n=3). D–F) Both bioengineered human pylorus and SI SMC constructs contracted in response to ACh with maximum contractions averaging 184.9 μN (SEM±5.66) and 172.1 μN (SEM±2.37), respectively (n=3). Contraction in response to ACh was abrogated with the addition of a muscarinic receptor inhibitor (atropine, red traces).

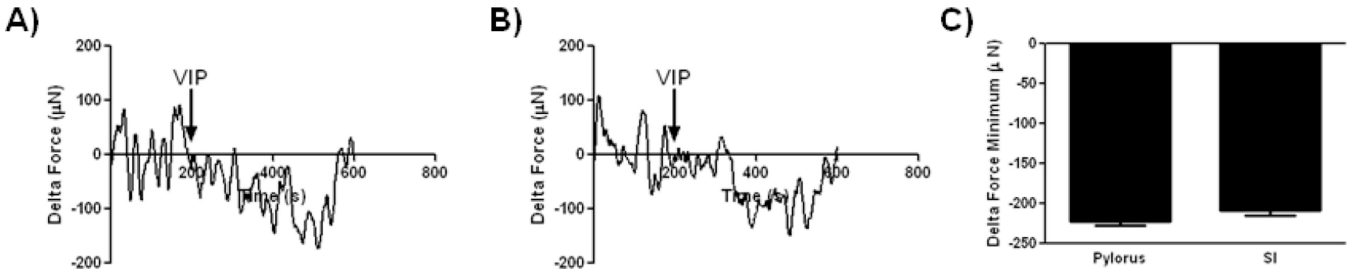

Figure 5. Physiologic assessment of force generation by bioengineered smooth muscle constructs in response to vasoactive intestinal peptide

Force of relaxation measurements were acquired by real time force generation measurements taken after stimulation of constructs with 1 μM VIP. A) Representative tracings of human pylorus SMC constructs are presented. Bioengineered human pylorus constructs relaxed in response to VIP averaging minimum forces of −228.8 μN (SEM±4.6). B) Human SI SMC constructs also relaxed in response to VIP averaging −208.6 μN (SEM ±6.8). C) No significant differences were observed in the maximum force of relaxation between bioengineered human pylorus and SI constructs (n=3).